The Role of Oxides in Catalytic CO Oxidation over Rhodium and Palladium

ACS Catalysis

Research Article

Cite This: ACS Catal. 2018, 8, 4438−4445

pubs.acs.org/acscatalysis

The Role of Oxides in Catalytic CO Oxidation over Rhodium and Palladium

Johan Gustafson,*[,†] Olivier Balmes,[‡] Chu Zhang,[†] Mikhail Shipilin,[¶] Andreas Schaefer,[§] Benjamin Hagman,[†] Lindsay R. Merte,[‡,∥] Natalia M. Martin,[§] Per-Anders Carlsson,[§] Maciej Jankowski,[⊥] Ethan J. Crumlin,[#] and Edvin Lundgren[†]

[†]Synchrotron Radiation Research, Lund University, Box 118, 221 00 Lund, Sweden

[‡]MAX IV Laboratory, Lund University, Box 118, 221 00 Lund, Sweden

[¶]Department of Physics, AlbaNova University Center, Stockholm University, 10691 Stockholm, Sweden

[§]Department of Chemistry and Chemical Engineering, Chalmers University of Technology, 412 96 Göteborg, Sweden

[∥]Department of Physics, Chalmers University of Technology, 412 96 Göteborg, Sweden

[⊥]European Synchrotron Radiation Facility, CS40220, 38043 CEDEX 9 Grenoble, France

[#]Advanced Light Source, Lawrence Berkeley National Laboratory, One Cyclotron Road, Berkeley, California 94720, United States

Supporting Information

ABSTRACT: Catalytic CO oxidation is a seemingly simple reaction between CO and O_2 molecules, one of the reactions in automotive catalytic converters, and the fruit-fly reaction in model catalysis. Surprisingly, the phase responsible for the catalytic activity is still under debate, despite decades of investigations. We have performed a simple but yet conclusive study of single crystal Rh and Pd model catalysts, resolving this controversy. For Rh, the oxygen-covered metallic surface is more active than the oxide, while for Pd, thin oxide films are at least as active as the metallic surface, but a thicker oxide is less active. Apart from resolving a long-standing debate, our results pinpoint important design principles for oxidation catalysts as to prevent catalytic extinction at high oxygen exposures.

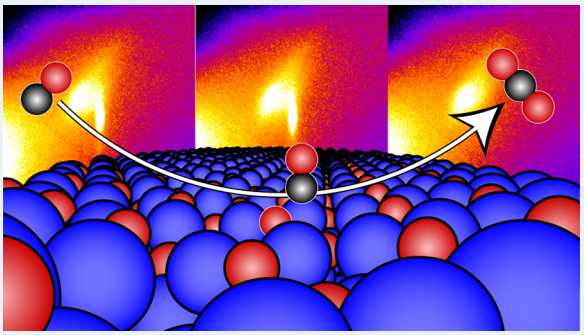

KEYWORDS: *CO oxidation, palladium, rhodium, oxide, surface oxide, oxidation catalysis, active phase*

INTRODUCTION

Because of the high complexity of industrial heterogeneous catalysts, a fundamental understanding of catalytic processes is in many cases missing. Such an understanding has become the main goal of surface-science-based catalysis research, and the importance of that approach has been strongly emphasized in the Science and Technology Roadmap on Catalysis for Europe prepared by the European Cluster on Catalysis.[1] Traditionally, such studies are done under highly simplified conditions, on single crystals in ultrahigh vacuum (UHV). Over the last decades, however, there has been a strong effort toward doing detailed surface science studies under more realistic conditions. In this context, catalytic CO oxidation by O_2 over Pt-group metals has, because of its industrial relevance and relative simplicity, become the fruit-fly reaction and a widely used reference model system for oxidation catalysis. Surprisingly, despite a lot of effort, there has been no consensus about the catalytic mechanism on the atomic level under realistic conditions.[2]

Under UHV conditions, it is well-established that the reaction can proceed on the metallic surface through the Langmuir−Hinshelwood mechanism. During adsorption on a suitable metal surface, such as Rh or Pd, the O_2 molecules dissociate spontaneously, and the major barrier for the reaction is removed. If CO is also adsorbed on the surface, it can react with atomic oxygen to form CO_2 that readily desorbs and closes the catalytic cycle (see the bottom of Figure 1).

At more realistic pressures, mixed adsorbate structures rarely form, but instead one of the reactants tends to dominate the surface completely. At low temperatures, the relatively high CO sticking probability favors adsorption of CO, which by far becomes the most abundant surface species. At high CO coverage, adsorbate structures form that effectively block the O_2 dissociation, and an O_2 molecule impinging on such a surface will most often leave unreacted (see left part of Figure 1). This surface is referred to as CO poisoned (and the phenomenon is referred to as CO self-poisoning) and associated with low catalytic activity. Increasing the temperature leads to an increased CO desorption rate and formation of vacant sites. These sites can either be filled by another (or the same) CO

Received: February 5, 2018
Revised: April 7, 2018
Published: April 10, 2018

DOI: 10.1021/acscatal.8b00498
ACS Catal. 2018, 8, 4438−4445

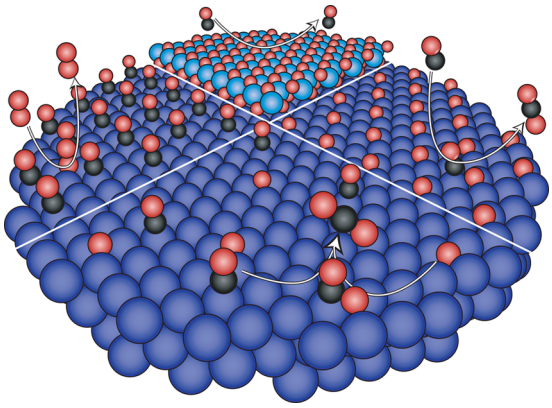

Figure 1. Different phases of the Rh(111) surface. During CO oxidation over Rh(111), four different phases are of interest. (Bottom) Metallic surface under high vacuum conditions with low coverage, where both CO and O_2 can adsorb and react to form CO_2. (Left) At moderate pressures and low temperatures, the surface is covered by CO, which hinders dissociative adsorption of O_2 and hence the reaction. (Right) At higher temperatures, the surface is covered by O, but there is still room for CO to adsorb (nondissociatively), resulting in an active surface. (Top) Under realistic conditions, a surface oxide might form, consisting of a trilayer with O−Rh−O. There is a debate in the literature concerning whether this surface oxide or the oxygen covered metallic surface (right) is the active phase.

molecule or by an O_2 molecule that now has space to dissociate. In the latter case, the resulting O atoms will soon react with neighboring CO molecules and leave an even larger proportion of the surface available for adsorption of CO or O_2. If the temperature is high enough, and the gas mixture has a sufficient excess of O_2, the freed area will mainly be filled by oxygen so that the reaction continues until all CO is removed from the surface. Adsorbed oxygen, however, cannot block the associative adsorption of CO, and hence, this surface possesses high catalytic activity (see right part of Figure 1).

Since the CO oxidation is an exothermic reaction, the transition from low to high active state is associated with a considerable heat release that leads to a self-acceleration of the reaction, the so-called catalytic ignition.[3] Analogously, the reverse transition is referred to as the extinction, which is accompanied by a temperature drop. For the ignited catalyst, the CO oxidation reaction is no longer determined by the intrinsic activity of the catalyst but by the transport of reactants to the catalytic surface, and thus, it is almost independent of temperature. This can either be referred to as the reaction being diffusion controlled or mass transfer limited (MTL). In such a situation, assuming, as above, that the reaction mixture has an excess of O_2, the gas composition close to the catalyst will be depleted in CO, and the surface will be exposed to an oxidizing atmosphere of O_2 and CO_2.[4,5]

Several in situ studies have, however, shown that both a chemisorbed oxygen phase and oxides may form in conjunction with the ignition,[2,6−14] suggesting that the oxides are responsible for the high activity. This idea is supported by a number of UHV-based studies, indicating that the formation of CO_2 through the reaction of gas-phase CO with oxide films is faster than with preadsorbed O on metallic surfaces.[15−19] Other studies, mainly based on infrared reflection absorption spectroscopy (IRAS), suggest that the active surface is metallic and that any oxide present is an almost inactive spectator phase, which, because the metal is so active, can almost completely cover the surface while the reaction is still in the MTL.[20−26] A very recent UHV investigation concludes that metallic Pd and PdO have a rather similar activity, but under the studied conditions, the metal is 2−3 times more active.[27]

In order to investigate the relative activity between the metal and the oxides, under realistic pressures, we have carefully followed the relation between surface structure and catalytic activity, using surface X-ray diffraction (SXRD), ambient-pressure X-ray photoelectron spectroscopy (APXPS), and mass spectrometry (MS) during extinction of the catalyst instead of the ignition.

Starting from a situation where the reaction is in the MTL and the surface is covered by an oxide, we slowly lower the temperature. This lowers the reaction rate until the MTL cannot be maintained, and the CO partial pressure near the surface will increase. This, in turn, leads to partial reduction of the oxide and exposure of metallic surface. If the metal is more active than the oxide, the reaction rate will increase. There will then be a new equilibrium situation, where a part of the surface will be metallic, while the rest is oxidized, and the reaction is once again in the MTL. As the temperature is lowered further, the equilibrium will gradually shift toward a larger part of the surface being metallic before the MTL is restored. Hence, **if the oxide is less active than the metal, the corresponding signal should gradually decrease** until the whole surface needs to be metallic in order to stay in the MTL, and further cooling will result in extinction. If the metal is *not* more active than the oxide, however, the exposure of more metal will not increase the reaction rate, and the reaction will stay in the low activity regime. That is, **if the oxide is at least as active as the metal, it will stay** on the surface until the reaction is slower than the transport of CO, and the extinction and removal of the oxide will coincide. Finally, **any additional structure that is present in the active state and does not disappear immediately after extinction would be significantly less active**. In contrast to what has generally been assumed, the Rh and Pd samples showed opposite behaviors with metallic Rh and thin Pd oxides being most active.

EXPERIMENTAL SECTION

The Rh(111) and Pd(100) single crystal surfaces (Surface Preparation Lab) were cleaned in a standard way by cycles of Ar^+ sputtering and subsequent annealing. By annealing the crystals in an O_2 pressure of 10^{-7} mbar, carbon contaminations could be removed, and any remaining oxygen could be removed by flashing at 800 °C in UHV. This procedure was repeated until no impurities could be detected by XPS or SXRD.

The SXRD measurements were performed in the in situ flow reactor chamber at the surface diffraction beamline ID03[28,29] at the European Synchrotron Radiation Facility (ESRF) in Grenoble, France. The wavelength of the incident X-rays was set to 0.517 Å. The sample was aligned according to the bulk Bragg reflections of each substrate. The coordinates (h, k, l) in reciprocal space refer to a basis ($\mathbf{a}^*$, $\mathbf{b}^*$, $\mathbf{c}^*$) with $\mathbf{a}^*$ and $\mathbf{b}^*$ spanning the reciprocal surface lattice of the substrate and $\mathbf{c}^*$ being perpendicular to the surface plane.

For Rh(111), $|\mathbf{a}^*| = |\mathbf{b}^*| = 2\pi/d_{112}$; $|\mathbf{c}^*| = 2\pi/\sqrt{3}a_0$ with a_0 = 3.80 Å (Rh bulk lattice constant); $d_{112} = a_0/2$; $\wedge_{\mathbf{a}^*,\mathbf{b}^*} = 60°$. The substrate and surface oxide signals were monitored at (h, k, l) = (0, 1, 0.3) and (0, 0.89, 0.3), respectively.

For Pd(100), $|\mathbf{a}^*| = |\mathbf{b}^*| = 2\pi/d_{110}$; $|\mathbf{c}^*| = 2\pi/a_0$ with a_0 = 3.89 Å (Pd bulk lattice constant); $d_{110} = a_0/\sqrt{2}$; $\wedge_{\mathbf{a}^*,\mathbf{b}^*} = 90°$.

DOI: 10.1021/acscatal.8b00498
ACS Catal. 2018, 8, 4438−4445

The surface oxide signal was monitored at $(h, k, l) = (0.8, 0.4, 0.74)$.

For the Pd bulk oxide data, a large ACSD detector was used, covering a range in reciprocal space of about $\sqrt{h^2 + k^2} = 0 - 3$ reciprocal lattice units (RLU) and $l = 0-2$ RLU. This enables us to follow the substrate CTR, epitaxial bulk oxide and polycrystalline oxide simultaneously. The substrate and epitaxial bulk oxide signals were monitored separately at around $(h, k, l) = (-2, 1, 0.5)$ and $(-1.4, 0.8, 0.6)$, respectively. The epitaxial and polycrystalline oxide signals were studied together around $(h, k, l) = (-1.6, 0.8, 1.4)$.

The APXPS data were recorded at beamline 9.3.2 at the ALS in Berkeley, CA,[30,31] where differential pumping and electrostatic lenses enable measurements in gas pressures up to 10 mbar. The gas mixture was controlled by leak valves. The sample was mounted on a special nonreactive sample holder in order not to interfere with the catalysis measurements. The O 1s and Pd $3d_{5/2}$ levels were measured using photon energies of 650 and 435 eV, respectively. The spectra were deconvoluted using a Doniach-Šunjić line shape convoluted with a Gaussian line shape. A linear background was also subtracted from the spectra. The spectra were calibrated using the Fermi edge.

RESULTS

Active Phase of Rh. Starting with the Rh(111) surface, Figure 2 shows an operando SXRD measurement following the surface oxide signal during extinction (marked with the vertical line) in a flow of 59, 33, and 8 mL_n/min (mL_n = mL at 1 atm and 0 °C) of O_2, CO and Ar, respectively, and a total pressure of 300 mbar. The constant CO_2 MS signal prior to extinction in Figure 2a shows that the catalytic activity here is in the MTL and not depending on the temperature. Simultaneously, the SXRD surface oxide signal in Figure 2b drops continuously, showing that more and more metal surface is needed in order to stay in the MTL. Hence, *the Rh metal is the active phase*.

The sudden drop in temperature in conjunction with the extinction shows that the reaction releases a significant amount of heat, as expected for the exothermal reaction.

Active Phase of Pd. Figure 3 shows a corresponding measurement on Pd(100), but with a flow of 2.5, 2.5, and 45 mL_n/min O_2, CO, and Ar, respectively, and a total pressure of 200 mbar. After activation at about 300 °C, these conditions resulted in a coexistence of two different bulk oxide structures; one thin that grows epitaxially to the substrate and one thicker that is polycrystalline (Figure 4b,c).[8] The response of the MS and temperature for this system is very similar to the Rh case, with a sudden deactivation of the catalyst, except that the temperature drop is less significant. The weaker response in the temperature is because the lower flow of reactants results in a lower reaction rate and a weaker heating effect from the exothermic reaction.

This measurement was done with a large 2D detector, enabling us to follow the oxide phases and the substrate Crystal Truncation Rod (CTR) simultaneously. Figure 3b shows the SXRD signal from two regions of interest, following the signal from the epitaxial oxide (blue) and the Pd(100) substrate CTR (red), respectively. Prior to the extinction, there are some intensity variations that we, because they appear in both the oxide and substrate signals, interpret as artifacts arising from small instabilities in the beam position. In conjunction with the extinction, however, the oxide signal disappears completely. There is no gradual drop in intensity, as found for Rh, showing

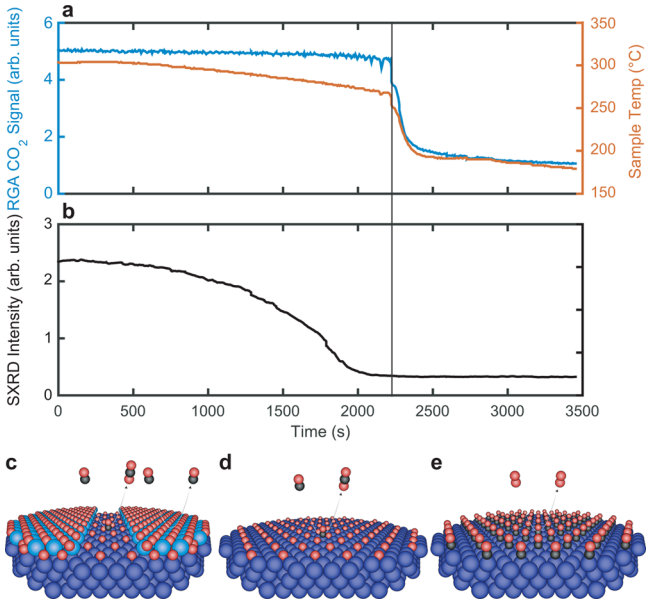

Figure 2. Active phase of Rh(111). The extinction of the CO oxidation reaction over Rh(111) is followed while slowly decreasing the sample temperature. (a) Mass spectrometry data (blue line) and sample temperature (red line) showing that in the beginning of the experiment, the CO_2 production is mass transfer limited and does not depend significantly on temperature. At a sample temperature of about 270 °C, however, the activity suddenly drops. (b) SXRD signal of the surface oxide showing that the oxide disappears gradually with decreasing sample temperature. This disappearance before the drop in catalytic activity shows that the metallic surface is more active than the surface oxide. (c–e) Models of the different phases present during the experiment. In the beginning, there is a surface oxide, but the reaction occurs on metallic areas between the oxide islands (c). Just before the reaction stops, the surface is completely metallic and covered by O (d). After extinction, the surface is covered by CO, which hinders dissociative adsorption of O_2 (e).

that *the epitaxial Pd oxide is at least as active as the metallic surface*.

The CTR signal mainly reflects how flat the interface between the substrate and the oxide or vacuum is. The interface gets slightly rougher during the reduction of the oxide, because of the deposition of the Pd that was formerly in the oxide structure, but it soon flattens out again and becomes slightly more well ordered than before the reduction.

Figure 3c shows a sequence of detector images around the time of the extinction, zoomed in such that the signals of the epitaxial as well as the polycrystalline oxides can be seen. The extinction occurred between the second and third images, at about t = 1704 s. As shown above, the epitaxial oxide disappears completely at this point, while the polycrystalline oxide is reduced much more slowly and is not completely gone until the last frame about 15 s after extinction. This shows that, in contrast to the epitaxial oxide, *the polycrystalline oxide is significantly less active*.

After activation of the Pd(100) model catalyst at the higher temperature of 400 °C, the resulting oxide film is the single-layer surface oxide (Figure 4a). Figure 5 shows the results from the corresponding extinction. The results are very similar to those from the epitaxial bulk oxide, with sudden extinction seen in MS and temperature in conjunction with the disappearance of the SXRD oxide signal. Therefore, we conclude that also *the Pd surface oxide is at least as active as the metallic surface*. Here,

DOI: 10.1021/acscatal.8b00498
ACS Catal. 2018, 8, 4438–4445

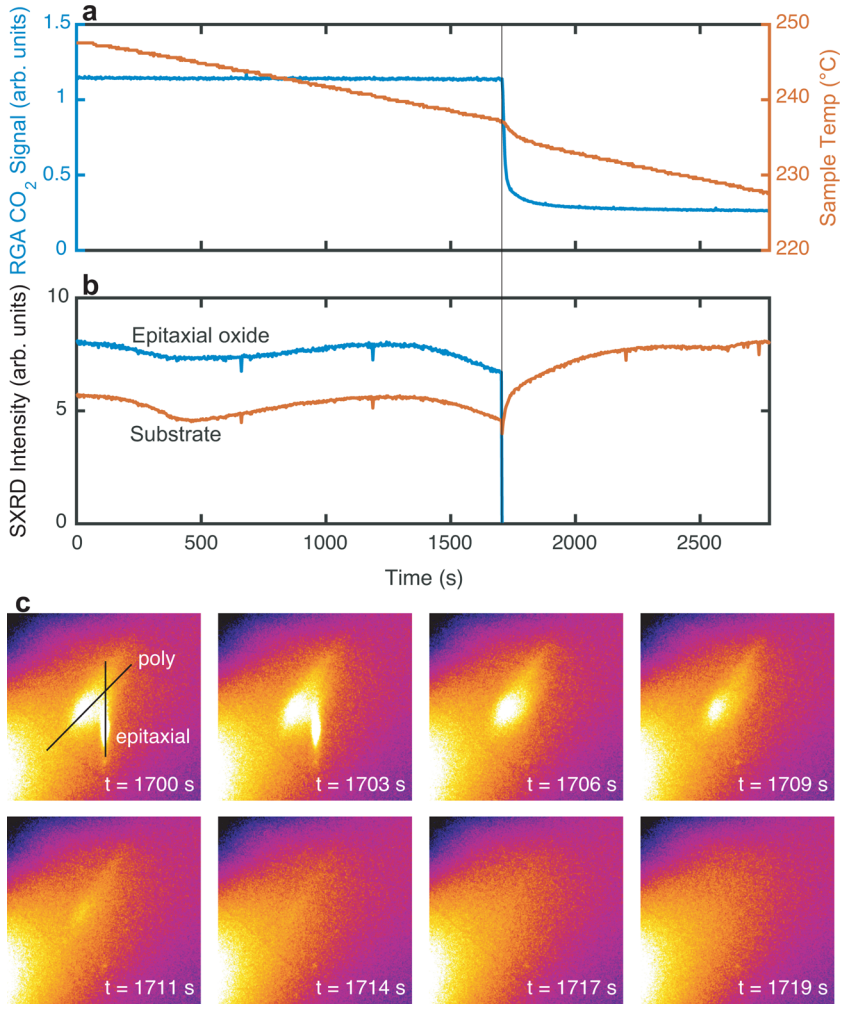

Figure 3. Activity of the bulk oxides on Pd(100). The extinction of the CO oxidation reaction over Pd(100), covered by bulk oxide, is followed while slowly decreasing the sample temperature. (a) Mass spectrometry data (blue line) and sample temperature (red line) showing that in the beginning of the experiments, the CO_2 production is mass transfer limited and does not depend significantly on temperature. At a sample temperature of about 235 °C, the activity suddenly drops. (b) SXRD signals from the epitaxial bulk oxide and the Pd(100) substrate CTR. The oxide signal stays close to unaffected until extinction, when it suddenly disappears, showing that the epitaxial oxide is at least as active as the metal. The similarity between the oxide and substrate CTR signals, prior to extinction, shows that the variations are not related to the amount of oxide on the surface, but rather small instabilities in the beam position. (c) These SXRD measurements were done using a large 2D detector, enabling us to follow the epitaxial and polycrystalline oxide phases simultaneously. Here, a series of detector images is shown, where both oxides can be seen and distinguished, from a time span of 19 s around the extinction point. The epitaxial oxide disappears suddenly with the catalytic activity, while the polycrystalline phase stays significantly longer, showing that it is significantly less active.

the gradual decrease in SXRD intensity before extinction is related to the mismatch between the surface oxide and the Pd substrate, as described further in the online Supporting Information.

The SXRD results for the Pd surface oxide are confirmed by the APXPS data in Figure 6, following the O 1s and Pd $3d_{5/2}$ levels in a 1:1 mixture of O_2 and CO at a total pressure of about 0.6 mbar during stepwise cooling. Under these conditions, APXPS reveals not only what is on the surface (solid lines), but also in the gas phase just above the surface (dotted lines). The Pd surface oxide is identified by two components in the O 1s spectrum, corresponding to oxygen in the oxide film, as well as a largely shifted Pd 3d component, due to the 4-fold oxygen coordinated Pd atoms in the oxide.

At temperatures above 220 °C, the O 1s spectra in Figure 6 display two gas-phase peaks corresponding to O_2,[32] and one corresponding to CO_2, showing that the sample is catalytically active. The CO signal is below the detection limit, showing that the catalytic activity is in the MTL and all the CO near the surface is immediately turned into CO_2. On the surface, we find a broad peak corresponding to surface oxygen, which is well fitted by two components in agreement with the surface oxide being present on the surface. In addition, there is a broad background from the Pd 3p level, which coincides with O 1s. The presence of the surface oxide is confirmed by the largely shifted component in the Pd 3d level. As compared to previously reported XPS data, from the surface oxide prepared in pure O_2, the component corresponding to 4-fold coordinated Pd atoms is relatively small, and in order to achieve a good fit of the data, another component had to be introduced, between the 2-fold and 4-fold components. We interpret this as 3-fold coordinated Pd that is present due to the ongoing reaction resulting in an equilibrium state between removal of O and reoxidation. Probably there is also one component corresponding to Pd coordinated to a single O

DOI: 10.1021/acscatal.8b00498
ACS Catal. 2018, 8, 4438−4445

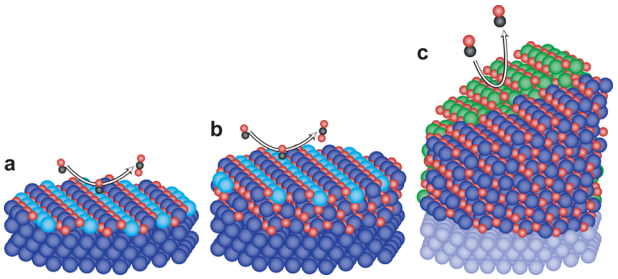

Figure 4. Models of the oxide structures on Pd(100). The surface oxide (a) and the thin epitaxial bulk oxide (b) expose the PdO(101) surface plane with Coordinatively UnSaturated (CUS) Pd atoms (light blue), which act as active sites. (c) When the oxide grows thick enough, it instead exposes the more stable (100) surface orientation, which does not have any CUS Pd atoms, and hence is less active. At the same time, it relaxes and looses its registry with the substrate. As a result, the oxide film breaks up in many crystallites with random orientation (illustrated by the blue and green Pd atoms), resulting in a powder-ring-like feature in the SXRD.

atom, which coincides with the main peak corresponding to metallic Pd.

At a sample temperature of 220 °C, the CO_2 signal was replaced by gas-phase CO, and the O on the surface was almost completely replaced by adsorbed CO. Obviously, the model catalyst has deactivated and is now in the CO poisoned state.

The exact analysis of the spectra are of minor importance for this study. The main point is that we identify the surface oxide during high activity, and because the spectra are identical until deactivation, within the error margins, the results are not compatible with a decreasing oxide coverage. Hence they confirm that the surface oxide is active.

DISCUSSION

Our measurements show that, for CO oxidation, the most active phase of Rh(111) is a metal surface, which under

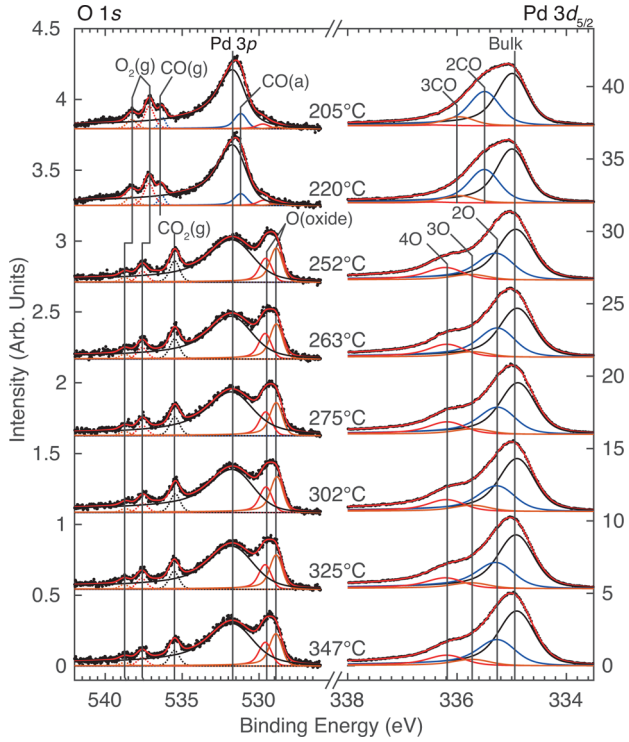

Figure 6. Confirming the activity of the surface oxide on Pd(100) with APXPS. O 1s and Pd $3d_{5/2}$ spectra measured during CO oxidation while stepwise reducing the temperature. The presence of the CO_2 gas phase peak and the absence of a corresponding CO peak shows that the catalyst is highly active until the extinction when the temperature goes below 250 °C. The split of the O 1s peak corresponding to oxygen on the surface, together with the largely shifted component in Pd $3d_{5/2}$, shows that the active surface is oxidized, and there is no significant change in the spectra until the extinction. This does not agree with an oxide phase with low activity that is gradually reduced while the temperature drops. Hence, the APXPS data confirms the SXRD results showing that the Pd surface oxide is active.

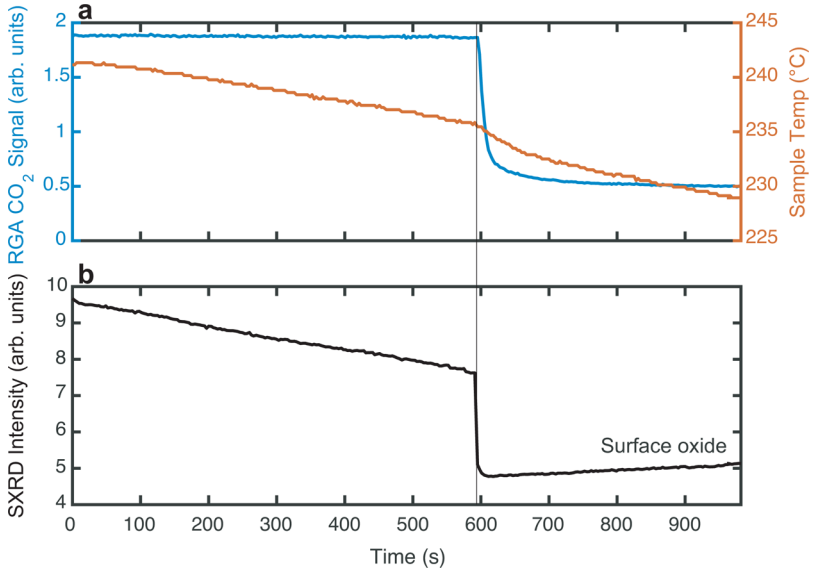

Figure 5. Activity of the surface oxide on Pd(100). The extinction of the CO oxidation reaction over Pd(100), covered by the surface oxide, is followed while slowly decreasing the sample temperature. (a) Mass spectrometry data (blue line) and sample temperature (red line) showing that in the beginning of the experiment, the CO_2 production is mass transfer limited and does not depend significantly on temperature. At a sample temperature of about 235 °C, the activity suddenly drops. (b) SXRD signals from the surface oxide, respectively. This oxide signal stays close to unaffected until extinction, when it suddenly disappears, showing that the surface oxide is at least as active as the metal.

DOI: 10.1021/acscatal.8b00498
ACS Catal. 2018, 8, 4438−4445

reaction conditions will be covered by chemisorbed oxygen. In contrast, the Pd surface oxide and a thin epitaxial PdO(101) film grown on Pd(100) are at least as active as metallic Pd, while only for a thick polycrystalline PdO film we find a lower activity. These results are rather surprising considering that previous studies have shown very similar results for Rh and Pd.

With these results in mind, however, we can reinterpret the results of previous studies without disagreements. At low temperatures, the surfaces are covered by CO, which poisons the reaction by inhibiting O_2 dissociation. When the temperature increases, the CO starts to desorb and the catalyst becomes active. At a certain temperature, the reaction ignites and the activity increases drastically. Several studies have shown that this coincides with the formation of oxides on the surface, but FTIR results by Zorn et al.[26] show that the surface stays metallic until the ignition. Not until the reaction has significantly increased the O_2:CO partial pressure ratio around the surface, the oxides may form. Hence, the oxides are not responsible for the change to high activity, but rather a result of it. This discussion is valid for Rh and Pd, as well as the other Pt-group metals. The present results, however, show that thin PdO films are more active than (or at least as active as) the Pd metal and can keep the high activity until a lower temperature. In contrast, a thick PdO film, as well as the surface oxide formed on Rh, are low-active phases.

At first sight, however, there seems to be a slight disagreement with the recent report by Weaver et al.,[27] which states that the metallic Pd(111) surface is 2−3 times more active for CO oxidation than the (101) surface of the epitaxial Pd oxide. In addition, it is found that the surface oxide, with a single PdO(101) layer, is significantly less active than the epitaxial bulk oxide. First of all, the error margins in our statement that the oxides are *at least as active* as the metal are possibly quite large. For instance, if the temperature drops too much during the initial reduction (see the Introduction), the reaction rate would not be high enough to reestablish the MTL even if the exposed metal is more active than the oxide. Similarly, the metal surface will be rather rough after reduction, because of the deposition of the Pd that was formerly in the oxide structure, which may lower the catalytic activity of the exposed metal surface.[33] Hence, what we can safely say is that the thin Pd oxides are not significantly less active than the metal and, although we have not been able to quantify this, we believe that a factor of 2−3 is too much.

In case there is a differences between the relative activities in our study and the one by Weaver et al., there are several plausible explanations. Most obvious is the fact that we studied Pd(100), whereas Weaver et al. studied Pd(111). Although the corresonding bulk oxides are the same, the surface oxides and the metallic surfaces will be slightly different. Further, the study by Weaver et al. was performed in UHV, while our measurements were done at pressures in the order of 100 mbar, close to realistic conditions for an industrial catalyst. Although the basic mechanisms would be expected to be similar, there might be differences. For instance, as the reaction on the oxide surface involves reduction and reoxidation of the oxide, the surface present during reaction will not be the perfect oxide, but rather an equilibrium structure, which depends heavily on the reaction gas mixture. In fact, our APXPS results show that, in addition to Pd atoms with 2- and 4-fold coordination to O, the active surface oxide exhibits 3- and possibly 1-fold coordinated Pd atoms.

The difference between Rh and Pd is most likely found in the surface structure of the corresponding oxides. Both the surface oxide and thicker oxide grown on Rh(111), have been found to expose fully oxygen terminated surfaces (see the top part of Figure 1), on which CO adsorbs very weakly.[34] The thin oxides on Pd(100), on the other hand, expose PdO(101) planes with Coordinatively UnSaturated (CUS) Pd atoms, where CO can adsorb (see Figure 4a,b).[17−19,35] These CUS atoms act as active sites for the reaction with O from the oxide structure. If the oxide grows thick enough, however, it loses its registry with the substrate and breaks up into several crystallites with random orientation (illustrated by the blue and green Pd atoms in Figure 4c), resulting in a powder-ring-like signal in SXRD. We expect these crystallites to expose (100) facets, as this has been predicted to be the most stable surface orientation of PdO without the presence of a Pd substrate.[35−37] In contrast to the (101) facet, the (100) does *not* expose any CUS Pd atoms, which explains the low activity of the thick Pd oxide.

CONCLUSIONS

To conclude, we have studied the activity for catalytic CO oxidation over Rh and Pd oxides under oxidizing conditions in CO and O_2 partial pressures in the order of 10−100 mbar. The results show that the Rh surface oxide shows low activity, while thin PdO(101) films grown on Pd(100) are at least as active toward CO oxidation as the metallic surface. Thicker PdO films, exposing the (100) plane, however, show low activity. The difference between the high- and low-activity oxides is that the highly active oxides expose CUS metal atoms that act as active sites.

These results are likely possible to generalize. The oxide formation has been found to be similar on all investigated Rh surfaces, including low-index and vicinal surfaces, as well as nanoparticles.[38−46] Similarly, surface oxides based on PdO(101) units have been reported for (100)[47−49] and (553)[50,51] surfaces of Pd, and on (100) and (111) facets, it has been shown that epitaxial bulk oxides with (101) surface orientation can form.[52−54] For further generalization, a RuO_2(110) oxide film, exposing CUS sites, is found to grow on Ru(0001), making it likely that the active phase of Ru is also oxidized, in agreement with the results of Over et al.[15,16] Pt, on the other hand, has been found to have a completely O terminated surface oxide, similar to Rh, and the Pt oxide would consequently be expected to show low activity. It has, however, been found that there is another structure forming on Pt(110) during high CO oxidation activity under moderately oxidizing conditions.[12] The corresponding structure is not properly determined, but a combined SXRD and DFT study suggests a structure that includes both O and C, and exposes CUS Pt atoms.

The present study resolves a long-standing debate concerning the active phase in CO oxidation. The knowledge about the activity of different oxide phases can have a major impact for dealing with some of the common problems with the oxidation catalysts of today. For instance, our results explain why Pd and Ru are less prone to oxygen poisoning (deactivation due to oxygen exposure) than for example Rh, which has oxides inhibiting CO adsorption.[55] Furthermore, our results can be used to decrease the effect of oxygen poisoning on Pd based catalysts even more. A bimetallic system where the PdO grows on top of another metal, which does not oxidize, might be able to stabilize the active (101) facet of the PdO film. In fact, PdAu bimetallic catalysts are reported being less sensitive to oxygen

DOI: 10.1021/acscatal.8b00498
ACS Catal. 2018, 8, 4438−4445

poisoning,[56,57] and possibly the limited thickness of the PdO film is part of the explanation.

■ ASSOCIATED CONTENT

Supporting Information

The Supporting Information is available free of charge on the ACS Publications website at DOI: 10.1021/acscatal.8b00498.

Further discussions on the use of the large 2D detector for SXRD and the misfit between the Pd surface oxide and the Pd(100) substrate (PDF)

■ AUTHOR INFORMATION

Corresponding Author

*E-mail: johan.gustafson@sljus.lu.se.

ORCID

Johan Gustafson: 0000-0003-3325-0658
Andreas Schaefer: 0000-0001-6578-5046
Natalia M. Martin: 0000-0002-6881-4989
Per-Anders Carlsson: 0000-0001-6318-7966
Maciej Jankowski: 0000-0002-3796-0529
Ethan J. Crumlin: 0000-0003-3132-190X
Edvin Lundgren: 0000-0002-3692-6142

Notes

The authors declare no competing financial interest.

■ ACKNOWLEDGMENTS

This work is done within the Röntgen-Ångström collaboration "Time-resolved *in situ* methods for design of catalytic sites within sustainable chemistry". The authors thank the Swedish Research Council, the Swedish Foundation for Strategic Research, the Crafoord Foundation and the Knut and Alice Wallenberg Foundation for financial support. The staff at the ESRF and the ALS are gratefully acknowledged. This research used resources of the Advanced Light Source, which is a DOE Office of Science User Facility under contract no. DE-AC02-05CH11231.

■ REFERENCES

(1) Centi, G.; Perathoner, S.; Gross, S.; Hensen, E. J. M. *Science and Technology Roadmap on Catalysis for Europe. A path to create a sustainable future*; ERIC aisbl Pub.: Bruxelles, Belgium, 2016.

(2) van Spronsen, M. A.; Frenken, J. W.; Groot, I. M. Surface science under reaction conditions: CO oxidation on Pt and Pd model catalysts. *Chem. Soc. Rev.* **2017**, *46*, 4347−4374.

(3) Frank-Kamenetskii, D. A. *Diffusion and heat exchange in chemical kinetics*; Princeton University Press: Princeton, NJ, 2015; pp 463−466.

(4) Matera, S.; Reuter, K. First-principles approach to heat and mass transfer effects in model catalyst studies. *Catal. Lett.* **2009**, *133*, 156.

(5) Zetterberg, J.; Blomberg, S.; Gustafson, J.; Evertsson, J.; Zhou, J.; Adams, E. C.; Carlsson, P.-A.; Aldén, M.; Lundgren, E. Spatially and temporally resolved gas distributions around heterogeneous catalysts using infrared planar laser-induced fluorescence. *Nat. Commun.* **2015**, *6*, 7076.

(6) Gustafson, J.; Westerström, R.; Resta, A.; Mikkelsen, A.; Andersen, J.; Balmes, O.; Torrelles, X.; Schmid, M.; Varga, P.; Hammer, B.; Kresse, G.; Baddeley, C.; Lundgren, E. Structure and catalytic reactivity of Rh oxides. *Catal. Today* **2009**, *145*, 227−235.

(7) Westerström, R.; Wang, J.; Ackermann, M.; Gustafson, J.; Resta, A.; Mikkelsen, A.; Andersen, J.; Lundgren, E.; Balmes, O.; Torrelles, X.; Frenken, J.; Hammer, B. Structure and reactivity of a model catalyst alloy under realistic conditions. *J. Phys.: Condens. Matter* **2008**, *20*, 184018.

(8) van Rijn, R.; Balmes, O.; Resta, A.; Wermeille, D.; Westerström, R.; Gustafson, J.; Felici, R.; Lundgren, E.; Frenken, J. Surface structure and reactivity of Pd(100) during CO oxidation near ambient pressures. *Phys. Chem. Chem. Phys.* **2011**, *13*, 13167−13171.

(9) van Rijn, R.; Balmes, O.; Felici, R.; Gustafson, J.; Wermeille, D.; Westerström, R.; Lundgren, E.; Frenken, J. W. Comment on "CO oxidation on Pt-group metals from ultrahigh vacuum to near atmospheric pressures. 2. Palladium and platinum. *J. Phys. Chem. C* **2010**, *114*, 6875−6876.

(10) Blomberg, S.; Hoffmann, M.; Gustafson, J.; Martin, N.; Fernandes, V.; Borg, A.; Liu, Z.; Chang, R.; Matera, S.; Reuter, K.; Lundgren, E. In situ x-ray photoelectron spectroscopy of model catalysts: At the edge of the gap. *Phys. Rev. Lett.* **2013**, *110*, 117601.

(11) Hendriksen, B.; Frenken, J. CO oxidation on Pt(110): scanning tunneling microscopy inside a high-pressure ow reactor. *Phys. Rev. Lett.* **2002**, *89*, 046101.

(12) Ackermann, M.; Pedersen, T.; Hendriksen, B.; Robach, O.; Bobaru, S.; Popa, I.; Quirós, C.; Kim, H.; Hammer, B.; Ferrer, S.; Frenken, J. Structure and reactivity of surface oxides on Pt(110) during catalytic CO oxidation. *Phys. Rev. Lett.* **2005**, *95*, 255505.

(13) Hendriksen, B.; Bobaru, S.; Frenken, J. Oscillatory CO oxidation on Pd(100) studied with in situ scanning tunneling microscopy. *Surf. Sci.* **2004**, *552*, 229−242.

(14) Hendriksen, B.; Bobaru, S.; Frenken, J. Bistability and oscillations in CO oxidation studied with scanning tunnelling microscopy inside a reactor. *Catal. Today* **2005**, *105*, 234−243.

(15) Over, H.; Kim, Y.; Seitsonen, A.; Wendt, S.; Lundgren, E.; Schmid, M.; Varga, P.; Morgante, A.; Ertl, G. Atomic-scale structure and catalytic reactivity of the RuO2(110) surface. *Science* **2000**, *287*, 1474−1476.

(16) Over, H.; Seitsonen, A. P.; Lundgren, E.; Schmid, M.; Varga, P. Direct imaging of catalytically important processes in the oxidation of CO over RuO2(110). *J. Am. Chem. Soc.* **2001**, *123*, 11807−11808.

(17) Zhang, F.; Li, T.; Pan, L.; Asthagiri, A.; Weaver, J. F. CO oxidation on single and multilayer Pd oxides on Pd(111): mechanistic insights from RAIRS. *Catal. Sci. Technol.* **2014**, *4*, 3826−3834.

(18) Zhang, F.; Pan, L.; Li, T.; Diulus, J. T.; Asthagiri, A.; Weaver, J. F. CO Oxidation on PdO (101) during Temperature-Programmed Reaction Spectroscopy: Role of Oxygen Vacancies. *J. Phys. Chem. C* **2014**, *118*, 28647−28661.

(19) Weaver, J. F.; Zhang, F.; Pan, L.; Li, T.; Asthagiri, A. Vacancy-Mediated Processes in the Oxidation of CO on PdO(101). *Acc. Chem. Res.* **2015**, *48*, 1515−1523.

(20) Chen, M.; Cai, Y.; Yan, Z.; Gath, K.; Axnanda, S.; Goodman, D. W. Highly active surfaces for CO oxidation on Rh, Pd, and Pt. *Surf. Sci.* **2007**, *601*, 5326−5331.

(21) Chen, M.; Wang, X. V.; Zhang, L.; Tang, Z.; Wan, H. Active surfaces for CO oxidation on palladium in the hyperactive state. *Langmuir* **2010**, *26*, 18113−18118.

(22) Gao, F.; Wang, Y.; Cai, Y.; Goodman, D. CO oxidation on Pt-group metals from ultrahigh vacuum to near atmospheric pressures. 2. Palladium and platinum. *J. Phys. Chem. C* **2009**, *113*, 174−181.

(23) Gao, F.; Cai, Y.; Gath, K.; Wang, Y.; Chen, M.; Guo, Q.; Goodman, D. CO oxidation on Pt-group metals from ultrahigh vacuum to near atmospheric pressures. 1. Rhodium. *J. Phys. Chem. C* **2009**, *113*, 182−192.

(24) Gao, F.; McClure, S.; Cai, Y.; Gath, K.; Wang, Y.; Chen, M.; Guo, Q.; Goodman, D. CO oxidation trends on Pt-group metals from ultrahigh vacuum to near atmospheric pressures: A combined in situ PM-IRAS and reaction kinetics study. *Surf. Sci.* **2009**, *603*, 65−70.

(25) McClure, S. M.; Goodman, D. W. New insights into catalytic CO oxidation on Pt-group metals at elevated pressures. *Chem. Phys. Lett.* **2009**, *469*, 1−13.

(26) Zorn, K.; Giorgio, S.; Halwax, E.; Henry, C. R.; Grönbeck, H.; Rupprechter, G. CO Oxidation on Technological Pd-Al2O3 Catalysts: Oxidation State and Activity. *J. Phys. Chem. C* **2011**, *115*, 1103−1111.

(27) Weaver, J. F.; Choi, J.; Mehar, V.; Wu, C. Kinetic coupling among metal and oxide phases during CO oxidation on partially-

DOI: 10.1021/acscatal.8b00498
ACS Catal. 2018, 8, 4438−4445

reduced PdO(101): Influence of gas-phase composition. *ACS Catal.* **2017**, *7*, 7319−7331.
(28) Balmes, O.; van Rijn, R.; Wermeille, D.; Resta, A.; Petit, L.; Isern, H.; Dufrane, T.; Felici, R. The ID03 surface diffraction beamline for in-situ and real-time X-ray investigations of catalytic reactions at surfaces. *Catal. Today* **2009**, *145*, 220−226.
(29) van Rijn, R.; Ackermann, M.; Balmes, O.; Dufrane, T.; Geluk, A.; Gonzalez, H.; Isern, H.; de Kuyper, E.; Petit, L.; Sole, V.; Wermeille, D.; Felici, R.; Frenken, J. Ultrahigh vacuum/high-pressure flow reactor for surface x-ray diffraction and grazing incidence small angle x-ray scattering studies close to conditions for industrial catalysis. *Rev. Sci. Instrum.* **2010**, *81*, 014101.
(30) Grass, M. E.; Karlsson, P. G.; Aksoy, F.; Lundqvist, M.; Wannberg, B.; Mun, B. S.; Hussain, Z.; Liu, Z. New ambient pressure photoemission endstation at Advanced Light Source beamline 9.3.2. *Rev. Sci. Instrum.* **2010**, *81*, 053106.
(31) Chang, R.; Hong, Y. P.; Axnanda, S.; Mao, B.; Jabeen, N.; Wang, S.; Tai, R.; Liu, Z. In-situ photoelectron spectroscopy with online activity measurement for catalysis research. *Curr. Appl. Phys.* **2012**, *12*, 1292−1296.
(32) Siegbahn, K.; Nordling, C.; Johansson, G.; Hedman, J.; Heden, P.; Hamrin, K.; Gelins, U.; Blergmark, T.; Werme, L.; Manne, R.; Baer, Y. *ESCA Applied to Free Molecules*; North-Holland: Amsterdam, 1969.
(33) Hendriksen, B. L.; Ackermann, M. D.; van Rijn, R.; Stoltz, D.; Popa, I.; Balmes, O.; Resta, A.; Wermeille, D.; Felici, R.; Ferrer, S.; Frenken, J. W. The role of steps in surface catalysis and reaction oscillations. *Nat. Chem.* **2010**, *2*, 730−734.
(34) Lundgren, E.; Gustafson, J.; Resta, A.; Weissenrieder, J.; Mikkelsen, A.; Andersen, J. N.; Köhler, L.; Kresse, G.; Klikovits, J.; Biederman, A.; Schmid, M.; Varga, P. The surface oxide as a source of oxygen on Rh(111). *J. Electron Spectrosc. Relat. Phenom.* **2005**, *144*, 367−372.
(35) Seriani, N.; Harl, J.; Mittendorfer, F.; Kresse, G. A first-principles study of bulk oxide formation on Pd(100). *J. Chem. Phys.* **2009**, *131*, 054701.
(36) Hellman, A.; Resta, A.; Martin, N.; Gustafson, J.; Trinchero, A.; Carlsson, P.-A.; Balmes, O.; Felici, R.; van Rijn, R.; Frenken, J.; Andersen, J.; Lundgren, E.; Grönbeck, H. The active phase of palladium during methane oxidation. *J. Phys. Chem. Lett.* **2012**, *3*, 678−682.
(37) Rogal, J.; Reuter, K.; Scheffler, M. Thermodynamic stability of PdO surfaces. *Phys. Rev. B: Condens. Matter Mater. Phys.* **2004**, *69*, 075421.
(38) Gustafson, J.; Mikkelsen, A.; Borg, M.; Lundgren, E.; Köhler, L.; Kresse, G.; Schmid, M.; Varga, P.; Yuhara, J.; Torrelles, X.; Quiros, C.; Andersen, J. Self-limited growth of a thin oxide layer on Rh(111). *Phys. Rev. Lett.* **2004**, *92*, 126102.
(39) Gustafson, J.; Mikkelsen, A.; Borg, M.; Andersen, J. N.; Lundgren, E.; Klein, C.; Hofer, W.; Schmid, M.; Varga, P.; Köhler, L.; Kresse, G.; Kasper, N.; Stierle, A.; Dosch, H. Structure of a thin oxide film on Rh(100). *Phys. Rev. B: Condens. Matter Mater. Phys.* **2005**, *71*, 115442.
(40) Gustafson, J.; Resta, A.; Mikkelsen, A.; Westerström, R.; Andersen, J. N.; Lundgren, E.; Weissenrieder, J.; Schmid, M.; Varga, P.; Kasper, N.; Torrelles, X.; Ferrer, S.; Mittendorfer, F.; Kresse, G. Oxygen-induced step bunching and faceting of Rh(553): Experiment and ab initio calculations. *Phys. Rev. B: Condens. Matter Mater. Phys.* **2006**, *74*, 035401.
(41) Dri, C.; Africh, C.; Esch, F.; Comelli, G.; Dubay, O.; Köhler, L.; Mittendorfer, F.; Kresse, G.; Dudin, P.; Kiskinova, M. Initial oxidation of the Rh(110) surface: ordered adsorption and surface oxide structures. *J. Chem. Phys.* **2006**, *125*, 094701.
(42) Klikovits, J.; Schmid, M.; Merte, L.; Varga, P.; Westerström, R.; Resta, A.; Andersen, J. N.; Gustafson, J.; Mikkelsen, A.; Lundgren, E.; Mittendorfer, F.; Kresse, G. Step-orientation-dependent oxidation: from 1D to 2D oxides. *Phys. Rev. Lett.* **2008**, *101*, 266104.
(43) Mittendorfer, F.; Seriani, N.; Dubay, O.; Kresse, G. Morphology of mesoscopic Rh and Pd nanoparticles under oxidizing conditions. *Phys. Rev. B: Condens. Matter Mater. Phys.* **2007**, *76*, 233413.
(44) Nolte, P.; Stierle, A.; Jin-Phillipp, N.; Kasper, N.; Schulli, T.; Dosch, H. Shape changes of supported Rh nanoparticles during oxidation and reduction cycles. *Science* **2008**, *321*, 1654−1658.
(45) Jin-Phillipp, N.; Nolte, P.; Stierle, A.; Dosch, H. Initial oxidation of MgO-supported Rh nanoparticles studied by TEM. *Surf. Sci.* **2009**, *603*, 2551−2555.
(46) Rupprechter, G.; Hayek, K.; Hofmeister, H. Electron microscopy of thin-film model catalysts: activation of alumina-supported rhodium nanoparticles. *J. Catal.* **1998**, *173*, 409−422.
(47) Todorova, M.; Lundgren, E.; Blum, V.; Mikkelsen, A.; Gray, S.; Gustafson, J.; Borg, M.; Rogal, J.; Reuter, K.; Andersen, J.; Scheffler, M. The Pd (100)−($\sqrt{5} \times \sqrt{5}$)R27°−O surface oxide revisited. *Surf. Sci.* **2003**, *541*, 101−112.
(48) Kostelník, P.; Seriani, N.; Kresse, G.; Mikkelsen, A.; Lundgren, E.; Blum, V.; Šikola, T.; Varga, P.; Schmid, M. The Pd(100)−($\sqrt{5} \times \sqrt{5}$)R27°−O surface oxide: A LEED, DFT and STM study. *Surf. Sci.* **2007**, *601*, 1574−1581.
(49) Shipilin, M.; Hejral, U.; Lundgren, E.; Merte, L. R.; Zhang, C.; Stierle, A.; Ruett, U.; Gutowski, O.; Skoglundh, M.; Carlsson, P.-A.; Gustafson, J. Quantitative surface structure determination using in situ high-energy SXRD: Surface oxide formation on Pd(100) during catalytic CO oxidation. *Surf. Sci.* **2014**, *630*, 229−235.
(50) Westerström, R.; Gustafson, J.; Resta, A.; Mikkelsen, A.; Andersen, J. N.; Lundgren, E.; Seriani, N.; Mittendorfer, F.; Schmid, M.; Klikovits, J.; Varga, P.; Ackermann, M.; Frenken, J.; Kasper, N.; Stierle, A. Oxidation of Pd(553): From ultrahigh vacuum to atmospheric pressure. *Phys. Rev. B: Condens. Matter Mater. Phys.* **2007**, *76*, 155410.
(51) Shipilin, M.; Gustafson, J.; Zhang, C.; Merte, L. R.; Lundgren, E. Step dynamics and oxide formation during CO oxidation over a vicinal Pd surface. *Phys. Chem. Chem. Phys.* **2016**, *18*, 20312−20320.
(52) Lundgren, E.; Gustafson, J.; Mikkelsen, A.; Andersen, J. N.; Stierle, A.; Dosch, H.; Todorova, M.; Rogal, J.; Reuter, K.; Scheffler, M. Kinetic hindrance during the initial oxidation of Pd(100) at ambient pressures. *Phys. Rev. Lett.* **2004**, *92*, 046101.
(53) Kan, H. H.; Weaver, J. F. A PdO(101) thin film grown on Pd(111) in ultrahigh vacuum. *Surf. Sci.* **2008**, *602*, L53−L57.
(54) Shipilin, M.; Gustafson, J.; Zhang, C.; Merte, L. R.; Stierle, A.; Hejral, U.; Ruett, U.; Gutowski, O.; Skoglundh, M.; Carlsson, P.-A.; Lundgren, E. Transient Structures of PdO during CO Oxidation over Pd(100). *J. Phys. Chem. C* **2015**, *119*, 15469−15476.
(55) Yao, Y.-F. Y. The oxidation of CO and hydrocarbons over noble metal catalysts. *J. Catal.* **1984**, *87*, 152−162.
(56) Jiang, H.-L.; Xu, Q. Recent progress in synergistic catalysis over heterometallic nanoparticles. *J. Mater. Chem.* **2011**, *21*, 13705−13725.
(57) Guo, Z.; Liu, B.; Zhang, Q.; Deng, W.; Wang, Y.; Yang, Y. Recent advances in heterogeneous selective oxidation catalysis for sustainable chemistry. *Chem. Soc. Rev.* **2014**, *43*, 3480−3524.

DOI: 10.1021/acscatal.8b00498
ACS Catal. 2018, 8, 4438−4445